Photophysics of Diimine Platinum(II) Bis-Acetylide Complexes

C. Ed Whittle,[†] Julia A. Weinstein,[‡] Michael W. George,[‡] and Kirk S. Schanze*[,†]

Department of Chemistry, University of Florida, P.O. Box 117200, Gainesville, Florida 32611-7200, and School of Chemistry, University of Nottingham, University Park, Nottingham, U.K. NG7 2RD

Received February 23, 2001

A comprehensive photophysical investigation has been carried out on a series of eight complexes of the type (diimine)Pt(−C≡C−Ar)$_2$, where diimine is a series of 2,2′-bipyridine (bpy) ligands and −C≡C−Ar is a series of substituted aryl acetylide ligands. In one series of complexes, the energy of the Pt → bpy metal-to-ligand charge transfer (MLCT) excited state is varied by changing the substituents on the 4,4′- and/or the 5,5′-positions of the bpy ligand. In a second series of complexes the electronic demand of the aryl acetylide ligand is varied by changing the para substituent (X) on the aryl ring (X = $-CF_3$, $-CH_3$, $-OCH_3$, and $-N(CH_3)_2$). The effect of variation of the substituents on the excited states of the complexes has been assessed by examining their UV−visible absorption, variable-temperature photoluminescence, transient absorption, and time-resolved infrared spectroscopy. In addition, the nonradiative decay rates of the series of complexes are subjected to a quantitative energy gap law analysis. The results of this study reveal that in most cases the photophysics of the complexes is dominated by the energetically low lying Pt → bpy ^{3}MLCT state. Some of the complexes also feature a low-lying intraligand (IL) $^3\pi,\pi^*$ excited state that is derived from transitions between π- and π^*-type orbitals localized largely on the aryl acetylide ligands. The involvement of the IL $^3\pi,\pi^*$ state in the photophysics of some of the complexes is signaled by unusual features in the transient absorption, time-resolved infrared, and photoluminescence spectra and in the excited-state decay kinetics. The time-resolved infrared difference spectroscopy indicates that Pt → bpy MLCT excitation induces a +25 to + 35 cm^{-1} shift in the frequency of the C≡C stretching band. This is the first study to report the effect of MLCT excitation on the vibrational frequency of an acetylide ligand.

Introduction

Transition metal complexes that feature metal-to-ligand charge transfer (MLCT) excited states have fascinated photochemists for four decades.[1−12] This fascination derives from a combination of features exhibited by MLCT excited states, which include visible light absorption, photoluminescence, long lifetimes, and relative inertness toward unimolecular photochemistry.[9] From the fundamental standpoint, MLCT excited states have provided considerable insight into nonradiative decay,[8,13,14] electron transfer processes,[7,15] solvent effects,[16,17] and small molecule−biopolymer interactions.[18] Moreover, recently MLCT excited states have become useful from a technological standpoint, finding application as sensitizers in dye-sensitized photovoltaic cells[19−21] and as luminescent reporters in optical gas sensors.[22−25]

By far the most work that has been carried out on MLCT states has focused on d^6 metal polypyridine complexes of Ru(II), Os(II), and Re(I).[8,9,13,14] However, recently there has been increasing interest in the properties of d^8 Pt(II) complexes of the type (diimine)PtL$_2$, where L = halide, nitrile, thiolate, isonitrile, and acetylide.[26−38] These Pt(II)−diimine complexes feature long-lived excited states that are believed to be based

* Corresponding author. E-mail: kschanze@chem.ufl.edu.
† University of Florida.
‡ University of Nottingham.

(1) Paris, J. P.; Brandt, W. W. *J. Am. Chem. Soc.* **1959**, *81*, 5001−5002.
(2) Demas, J. N.; Crosby, G. A. *J. Mol. Spectrosc.* **1968**, *26*, 72−77.
(3) Hager, G. D.; Crosby, G. A. *J. Am. Chem. Soc.* **1975**, *97*, 7031−7037.
(4) Hager, G. D.; Watts, R. J.; Crosby, G. A. *J. Am. Chem. Soc.* **1975**, *97*, 7037−7042.
(5) Hipps, K. W.; Crosby, G. A. *J. Am. Chem. Soc.* **1975**, *97*, 7042−7048.
(6) Van Houten, J.; Watts, R. *J. Am. Chem. Soc.* **1976**, *98*, 4853−4858.
(7) Meyer, T. J. *Prog. Inorg. Chem.* **1983**, *30*, 389−440.
(8) Caspar, J. V.; Meyer, T. J. *J. Phys. Chem.* **1983**, *87*, 952−957.
(9) Juris, A.; Balzani, V.; Barigelletti, F.; Campagna, S.; Belser, P.; von Zelewsky, A. *Coord. Chem. Rev.* **1988**, *84*, 85−277.
(10) Yeh, A. T.; Shank, C. V.; McCusker, J. K. *Science* **2000**, *289*, 935−938.
(11) Wrighton, M.; Morse, D. L. *J. Am. Chem. Soc.* **1974**, *96*, 998−1003.
(12) Lees, A. J. *Chem. Rev.* **1987**, *87*, 711−743.
(13) Caspar, J. V.; Kober, E. M.; Sullivan, B. P.; Meyer, T. J. *J. Am. Chem. Soc.* **1982**, *104*, 630−631.
(14) Worl, L. A.; Duesing, R.; Chen, P.; Della Ciana, L.; Meyer, T. J. *J. Chem. Soc., Dalton Trans.* **1991**, 849−858.
(15) Schanze, K. S.; Walters, K. A. In *Organic and Inorganic Photochemistry*; Ramamurthy, V., Schanze, K. S., Eds.; Molecular and Supramolecular Photochemistry, 2; Marcel-Dekker: New York, 1998; pp 75−128.
(16) Kozik, M.; Sutin, N.; Winkler, J. R. *Coord. Chem. Rev.* **1990**, *97*, 23−34.
(17) Chen, P. Y.; Meyer, T. J. *Chem. Rev.* **1998**, *98*, 1439−1477.
(18) Erkkila, K. E.; Odom, D. T.; Barton, J. K. *Chem. Rev.* **1999**, *99*, 2777−2795.
(19) Hagfeldt, A.; Gratzel, M. *Chem. Rev.* **1995**, *95*, 49−68.
(20) Grätzel, M.; O'Regan, B. *Nature* **1998**, *353*, 737−740.
(21) Argazzi, R.; Bignozzi, C. A.; Heimer, T. A.; Castellano, F. N.; Meyer, G. J. *J. Am. Chem. Soc.* **1995**, *117*, 11815−11816.
(22) Xu, W. Y.; McDonough, R. C.; Langsdorf, B.; Demas, J. N.; Degraff, B. A. *Anal. Chem.* **1994**, *66*, 4133−4141.
(23) Xu, W. Y.; Kneas, K. A.; Demas, J. N.; DeGraff, B. A. *Anal. Chem.* **1996**, *68*, 2605−2609.
(24) Schwab, S. D.; Levy, R. L. Formulations and Method of Use of Pressure Sensitive Paint. U.S. Patent 5,612,492, 1997.
(25) Schanze, K. S.; Carroll, B. F.; Korotkevitch, S.; Morris, M. J. *AIAA J.* **1997**, *35*, 306−310.
(26) Miskowski, V. M.; Houlding, V. H. *Inorg. Chem.* **1989**, *28*, 1529−1533.
(27) Kunkely, H.; Vogler, A. *J. Am. Chem. Soc.* **1990**, *112*, 5625−5627.
(28) Miskowski, V. M.; Houlding, V. H.; Che, C. M.; Wang, Y. *Inorg. Chem.* **1993**, *32*, 2518−2524.
(29) Chan, C. W.; Cheng, L. K.; Che, C. M. *Coord. Chem. Rev.* **1994**, *132*, 87−97.

10.1021/ic0102182 CCC: $20.00
Published on Web 07/04/2001

Chart 1

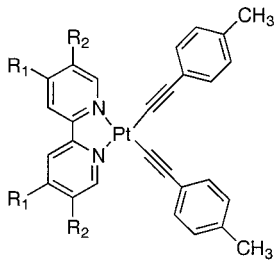

1a : $R_1 = R_2 = CH_3$
1b : $R_1 = C(CH_3)_3$, $R_2 = H$
1c : $R_1 = C(O)NEt_2$, $R_2 = H$
1d : $R_1 = CO_2Et$, $R_2 = H$

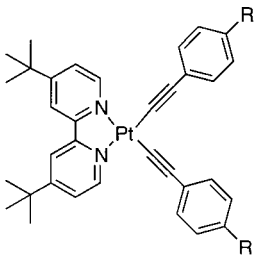

2a : $R = CF_3$
2b : $R = NO_2$
2c : $R = NMe_2$
2d : $R = OCH_3$

on dπ Pt $\rightarrow$ π^* diimine MLCT. In particular, in a recent study Eisenberg and co-workers examined the properties of a series of complexes of the type (diimine)Pt($-C\equiv C-Ar)_2$, where diimine is a substituted 1,10-phenanthroline or a 2,2′-bipyridine ligand and $-C\equiv C-Ar$ is an aryl-substituted acetylide ligand.[34,36] This group demonstrated that the (diimine)Pt($-C\equiv C-Ar)_2$ complexes feature a moderately intense absorption band in the blue and a strongly Stokes shifted emission arising from the Pt $\rightarrow$ diimine MLCT state. Consistent with the MLCT assignment, the absorption and emission energies decreased by substitution of electron-withdrawing groups on the diimine acceptor ligand.[36]

Concomitant with the Eisenberg group's work, we were engaged in a photophysical study of the series of (diimine)Pt($-C\equiv C-Ar)_2$ complexes **1a**−**d** and **2a**−**d** (Chart 1). The objective of this effort was to systematically examine the influence of the electronic demand of the diimine and aryl acetylide ligands on the properties of the MLCT excited state. Specifically, we wished to investigate whether a correlation exists between the energy of the MLCT excited state and the nonradiative decay rate (k_{nr}). In addition, we sought to characterize the spectroscopy of the excited state by using variable-temperature luminescence, transient absorption, and time-resolved infrared spectroscopy. The present paper comprises a report of our photophysical investigation on this series of complexes. Although three of the eight complexes that we examined were characterized in the earlier study,[36] the present investigation extends the previous work in several ways. First, by using the series of substituted 2,2′-bipyridine ligands, we are able to vary the energy of the Pt $\rightarrow$ diimine MLCT state by approximately 4000 cm^{-1} (0.5 eV). This energy range is considerably larger than that afforded by the series of substituted phenanthroline complexes examined previously.[36] Given this larger energy gap, it becomes possible to examine the quantitative energy gap law correlation and compare it to correlations observed for MLCT excited states in other families of complexes.[8,13] Second, the work described herein also characterizes the UV−visible excited-state absorption of the MLCT excited states. Most of the complexes feature excited-state absorptions that are consistent with the MLCT assignment. However, the difference absorption spectra of complexes **2a** and **2b** are distinct from those of the other members of the series, suggesting that in these complexes the lowest excited state is not MLCT. Third, this paper reports the infrared difference spectrum in the region of the C≡C stretch for the excited-state complexes **1a**, **1b**, and **2b**. This the first study to examine the influence of MLCT (or π,π^*) excitation on the vibrational spectrum of a metal−acetylide complex.

Experimental Section

Photophysical Measurements. Spectroscopic experiments were carried out either in CH_2Cl_2 or in 2-methyltetrahydrofuran (2-MTHF), and these solvents were purified by distillation from CaH_2 and Na/benzophenone, respectively. Spectroscopy carried out at room temperature was performed using samples that were degassed by argon purging for 20 min. Low-temperature spectroscopic experiments were carried out on samples that were degassed by four repeated freeze−pump−thaw cycles on a high-vacuum line. UV−visible absorption spectra were obtained on a Cary 100 instrument. All photophysical experiments (except for time-resolved infrared specroscopy, see below) were carried out with sample concentrations in the range 2−20 μM. At these low concentrations, the lifetimes were not concentration dependent (i.e., self-quenching is not a significant decay pathway).[34] For example, within experimental error the emission lifetime of **1a** was invariant over the concentration range 2−50 μM.

Steady-state photoluminescence spectroscopy was carried out on a SPEX Fluorolog 2 instrument. Emission spectra were corrected by using correction factors generated in-house with a standard calibration lamp. Sample concentrations were sufficiently low such that the absorbance at all wavelengths was <0.2 (typical concentration = 5×10^{-6} M). Photoluminescence quantum yields were determined relative to $Ru(bpy)_3^{2+}$ in water ($\Phi_{em} = 0.055$),[39] and appropriate corrections were made for the difference in refractive index of the sample and reference solutions. Low-temperature photoluminescence experiments were carried out with samples contained in an LN2 cooled optical cryostat (Oxford Instrument, DN-1704) connected to an Omega CYC3200 temperature controller.

Photoluminescence decay lifetimes were determined by time-correlated single photon counting on an instrument that was constructed in-house. Excitation was provided either by a blue diode laser (λ = 405 nm, nanoLED-07, IBH, Glasgow, U.K.) or by a near-UV light-emitting diode (λ = 370 nm, nanoLED-03, IBH, Glasgow, U.K.) operating at a 100 kHz repetition rate. Emission light was filtered by using interference filters (10 nm bandpass, λ_{em} = 500, 550, 600, or 650 nm, as appropriate). Photoluminescence decay times were determined by using the DECAN fluorescence deconvolution software.[40]

Transient absorption spectroscopy was carried out on an instrument that has been described previously.[41] Samples were contained in a cell that holds a total volume of 10 mL, and the contents were continuously recirculated through the pump−probe region of the cell. Samples were degassed by argon purging for 30 min. Excitation was provided by the third harmonic output of a Nd:YAG laser (355 nm, Spectra Physics, GCR-14). Typical pulse energies were 5 mJ·pulse^{-1}, which corresponded to an irradiance in the pump−probe region of 20 mJ·cm^{-2}. Artifacts caused by photoluminescence were corrected by using a data collection cycle that subtracts the transient signal obtained with the probe light blocked from the signal obtained with the probe light present. Transient absorption decay lifetimes were determined from

(30) Cummings, S. D.; Eisenberg, R. *J. Am. Chem. Soc.* **1996**, *118*, 1949−1960.
(31) Zhang, Y.; Ley, K. D.; Schanze, K. S. *Inorg. Chem.* **1996**, *35*, 7102−7110.
(32) Connick, W. B.; Gray, H. B. *J. Am. Chem. Soc.* **1997**, *119*, 11620−11627.
(33) Paw, W.; Cummings, S. D.; Mansour, M. A.; Connick, W. B.; Geiger, D. K.; Eisenberg, R. *Coord. Chem. Rev.* **1998**, *171*, 125−150.
(34) Connick, W. B.; Geiger, D.; Eisenberg, R. *Inorg. Chem.* **1999**, *38*, 3264−3265.
(35) Connick, W. B.; Miskowski, V. M.; Houlding, V. H.; Gray, H. B. *Inorg. Chem.* **2000**, *39*, 2585−2592.
(36) Hissler, M.; Connick, W. B.; Geiger, D. K.; McGarrah, J. E.; Lipa, D.; Lachiocotte, R. J.; Eisenberg, R. *Inorg. Chem.* **2000**, *39*, 447−457.
(37) Hissler, M.; McGarrah, J. E.; Connick, W. B.; Geiger, D. K.; Cummings, S. D.; Eisenberg, R. *Coord. Chem. Rev.* **2000**, *208*, 115−137.
(38) Adams, C. J.; James, S. L.; Liu, X. M.; Raithby, P. R.; Yellowlees, L. J. *J. Chem. Soc., Dalton Trans.* **2000**, 63−67.
(39) Harriman, A. *J. Chem. Soc., Chem. Commun.* **1977**, 777−778.
(40) Boens, N.; De Roeck, T.; Dockx, J.; DeSchryver, F. C. *DECAN*, 1.0 ed.; Leuven, BE, 1991.
(41) Wang, Y. S.; Schanze, K. S. *Chem. Phys.* **1993**, *176*, 305−319.

Table 1. Photophysical Parameters for Platinum Acetylide Complexes[a]

complex	λ_{abs}/nm	ϵ_{max}/M^{-1} cm^{-1}	λ_{em}/nm	ΔE_s/cm^{-1} [b]	Φ_{em}[c]	τ_{em}/ns[d]	$k_r/10^5$ s^{-1} [e]	$k_{nr}/10^6$ s^{-1} [f]	τ_{TA}/ns[g]
1a	294	43200	553	1150	0.27	1300	2.08	0.562	1285
	379	9000							
1b	286	45200	570	2400	0.113	800	1.41	1.11	793
	386	8500							
1c	294	57300	642	2480	0.007	103	0.68	9.64	100
	424	4500							
1d	268	28800	670	2350	0.0046	20	2.30	49.8	22
	291 (sh)	21000							
	309 (sh)	16500							
	445	5500							
2a	294	67200	538	1950	0.207	607	3.41	1.31	600
	389	12400							
2b	288	22600	561	650	0.0899	3600	0.25	0.253	3720
	305 (sh)	18700							
	323	27000							
	371	42000							
2c	300	49000	586	−600	0.0075	250	0.30	3.97	246
	454	6100							
2d	292	41800	623	2900	0.019	60	3.17	16.4	51
	401	7500							

[a] Argon-degassed CH_2Cl_2 solutions. [b] Thermally induced Stokes shift ($\Delta E_s = E_{00}(77\ K) - E_{00}(298\ K)$). [c] Emission quantum yield relative to $Ru(bpy)_3^{2+}$ actinometer ($\Phi_{em}(H_2O) = 0.057$).[39] [d] Emission decay lifetime. [e] Radiative decay rate, computed by $k_r = \Phi_{em}/\tau_{em}$. [f] Nonradiative decay rate, computed by $k_{nr} = (1 - \Phi_{em})/\tau_{em}$. [g] Decay lifetime of transient absorption.

the multiwavelength difference-absorption data by using the SPECFIT/32 factor analysis software.[42]

Time-resolved infrared measurements were performed using a step-scan FTIR interferometer. A detailed description of the Nottingham time-resolved step-scan FTIR (s^2-FTIR) apparatus is given elsewhere.[43] Briefly, the apparatus consists of a commercially available step-scan FTIR spectrometer (Nicolet Magna 860) equipped with a 100 MHz 12-bit digitizer and a 50 MHz MCT detector interfaced to a Nd:YAG laser (Spectra Physics GCR 12). Synchronization of the Nd:YAG laser with data collection was achieved by means of a pulse generator (Stanford DG535). In some experiments the signal was passed through a low-noise preamplifier (Stanford Research System, model SR560) which has been set up at 1 MHz for these experiments. Experiments at 77 K were performed in a home-built two-window cryogenic IR cell, with CaF_2 windows and Teflon spacers regulating the path length.[44] Sample concentrations were ≈1 mM for the s^2-FTIR experiments. Under these conditions the excited-state lifetime of **1a** was shorter than observed by emission decay kinetics, presumably due to concentration quenching.[34]

Synthesis. 4-Ethynyltoluene was purchased (Aldrich Chemical) and was used as received. 4-Nitrophenylacetylene,[45] 4-methoxyphenylacetylene,[46,47] 4-(trifluoromethyl)phenylacetylene[47] and 4-(*N*,*N*-dimethylamino)phenylacetylene[48] were prepared according to literature methods. The substituted 2,2′-bipyridine ligands were also prepared according to literature procedures.[49] The necessary (diimine)$PtCl_2$ complexes were prepared by reaction of K_2PtCl_4 with the substituted bipyridine in refluxing aqueous HCl solution.[36]

All of the (diimine)Pt(C≡C−Ar)$_2$ complexes were synthesized by reaction of the corresponding (diimine)$PtCl_2$ with the suitably substituted acetylenes, Ar−C≡C−H, according to the method described by James and co-workers.[50] The crude complexes were purified by chromatography on alumina using CH_2Cl_2 as the eluant. The purified complexes were fully characterized by ^{1}H NMR, ^{13}C NMR, and high-resolution mass spectroscopy. Complexes **1b**, **2b**, and **2d** were reported previously, and our spectroscopic data match those reported in the literatrure.[36] Spectral data for the new (diimine)Pt(C≡C−Ar)$_2$ complexes is listed below.

1a. ^{1}H NMR ($CDCl_3$, TMS): δ 9.41 (s, 2H), 7.75 (s, 2H), 7.42 (d, 4H), 7.07 (d, 4H), 2.39 (s, 6H), 2.37 (s, 6H), 2.36 (s, 6H). ^{13}C NMR (CD_2Cl_2): δ 150.85, 139.96, 136.92, 132.31, 128.96, 124.10, 123.95, 120.82, 112.24, 102.03, 90.48, 21.83, 20.53, 17.43 ppm. HRMS: calcd for $C_{32}H_{30}N_2Pt$ 637.206, found 637.205 [M + H].

1c. ^{1}H NMR ($CDCl_3$, TMS): δ 9.63 (d, 2H), 7.95 (s, 2H), 7.41 (d, 2H), 7.38 (d, 4H), 7.06 (d, 4H), 3.54 (q, 4H), 3.33 (q, 4H), 2.35 (s, 6H), 1.24 (t, 6H), 1.09 (t, 6H). ^{13}C NMR (CD_2Cl_2): δ 166.91, 156.73, 151.35, 146.56, 135.25, 131.62, 128.68, 125.15, 124.24, 121.06, 101.94, 85.68, 43.38, 39.51, 21.31, 14.32, 12.67. HRMS: calcd for $C_{38}H_{40}N_4O_2Pt$ 779.280, found 780.288 [M + H].

1d. ^{1}H NMR ($CDCl_3$, TMS): δ 9.98 (d, 2H), 8.62 (s, 2H), 8.07 (d, 2H), 7.36 (d, 4H), 7.07 (d, 4H), 4.47 (q, 4H), 2.35 (s, 6H), 1.43 (q, 6H). ^{13}C NMR (CD_2Cl_2, TMS): δ 163.88, 156.52, 152.55, 139.76, 135.56, 132.21, 128.72, 127.38, 125.13, 122.63, 85.85, 81.31, 63.21, 21.59, 14.40 ppm. HRMS: calcd for $C_{34}H_{30}N_2O_4Pt$ 725.185, found 726.193 [M + H]

2a. ^{1}H NMR ($CDCl_3$): δ 9.62 (d, 2H), 7.97 (s, 2H), 7.62 (m, 6H), 7.43 (d, 4H), 1.42 (s, 18H). (This compound was not sufficiently soluble to allow acquisition of ^{13}C NMR.) HRMS: calcd for $C_{36}H_{32}F_6N_2Pt$ 801.212, found 802.2191 [M + H].

2c. ^{1}H NMR ($CDCl_3$, TMS): δ 9.78 (broad s, 2H), 7.92 (s, 2H), 7.51 (d, 2H), 7.43 (d, 4H), 6.64 (d, 4H), 2.93 (s, 12H), 1.43 (s, 18H). ^{13}C NMR (CD_2Cl_2): δ 162.80, 156.23, 151.20, 148.42, 132.90, 124.42, 118.50, 116.99, 112.13, 102.23, 82.39, 40.69, 35.70, 30.23 ppm. HRMS: calcd for $C_{38}H_{44}N_4Pt$ 751.3214, found 751.3227.

Results and Discussion

Structures. This study examines the photophysical properties of the two series of (diimine)Pt(−C≡C−Ar)$_2$ complexes shown in Chart 1. In the first series, **1a**−**d**, the substituents on the diimine acceptor ligand are varied while the structure of the two acetylene ligands is held constant. Variation of these substituents has a strong effect on the energy of the LUMO of

(42) Binstead, R. A. *SPECFIT/32*, 1.0 ed.; Spectrum Software Associates: Chapel Hill, NC, 2000.
(43) Sun, X.-Z.; Colley, C. S.; Nikiforov, S. N.; Yang, J.; George, M. W. *Appl. Spectrosc.*, in press.
(44) George, M. W. Ph.D. Dissertation, University of Nottingham, Nottingham, U.K., 1990.
(45) Takahashi, S.; Kuroyama, Y.; Sonogashira, K.; Hagihara, N. *Synthesis* **1980**, 627−630.
(46) Hundertmark, T.; Littke, A. F.; Buchwald, S. L.; Fu, G. C. *Org. Lett.* **2000**, *2*, 1729−1731.
(47) Crisp, G. T.; Flynn, B. L. *J. Org. Chem.* **1993**, *58*, 6614−6619.
(48) Leonard, K. A.; Nelen, M. I.; Anderson, L. T.; Gibson, S. L.; Hilf, R.; Detty, M. R. *J. Med. Chem.* **1999**, *42*, 3942−3952.
(49) Cook, M. J.; Lewis, A. P.; McAuliffe, G. S. G.; Skarda, V.; Thomson, A. J.; Glasper, J. L.; Robbins, D. J. *J. Chem. Soc., Perkin Trans. 2* **1984**, 1293−1301.
(50) James, S. L.; Younus, M.; Raithby, P. R.; Lewis, J. *J. Organomet. Chem.* **1997**, *543*, 233−235.

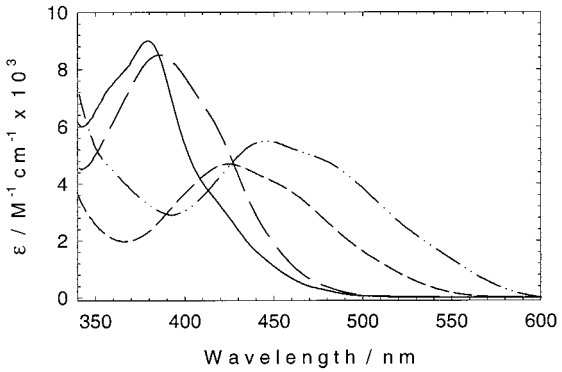

Figure 1. UV−visible absorption spectra of **1a**−**d** in CH_2Cl_2 solution. (—) **1a**; (− −) **1b**; (- - -) **1c**; (—··—) **1d**.

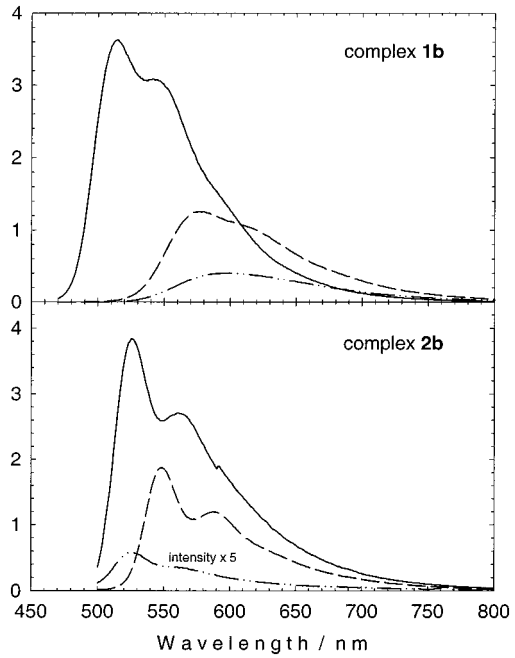

Figure 2. Photoluminescence spectra of **1b** (top) and **2b** (bottom) in 2-MTHF solution. In order of increasing intensity: 298, 140, and 80 K. The intensity of spectrum **2b** at 298 K is increased 5-fold to make it visible on the same scale.

the diimine acceptor ligand, which in turn is expected to exert a profound effect on the energy of the metal → diimine MLCT state as demonstrated in previous studies of Ru(II) and Re(I) complexes.[9,14] In the second series, **2a**−**d**, the diimine ligand is held constant (4,4′-bis(*tert*-butyl)-2,2′-bipyridine) while the para substituent on the arylacetylene ligand is varied. Variation of this substituent is anticipated to exert an effect on both the σ- and π-donor (or acceptor) properties of the acetylide ligands.

UV−Visible Absorption Spectroscopy. The (diimine)Pt(−C≡C−Ar)$_2$ complexes feature an array of absorptions in the UV−visible region that are due to a combination of intraligand (IL) π,π^* and MLCT transitions. Table 1 summarizes the band maxima and molar absorptivities for the transitions, and Figure 1 shows the long-wavelength region of the spectra for complexes **1a**−**d**. In general, all of the complexes feature moderately intense absorptions ($\epsilon < 10^4$ M^{-1} cm^{-1}) in the 350−500 nm region that arise from Pt → diimine MLCT. In addition, almost all of the complexes feature an intense band in the 290−310 nm region ($\epsilon \approx 5 \times 10^4$ M^{-1} cm^{-1}) which is clearly due to the π,π^* IL transitions. In general, the absorption features observed for the new complexes are in accord with those reported previously.[36]

Table 2. Emission Spectral Fitting Parameters[a]

complex	E_{00}/cm^{-1}	$\hbar\omega_m$/cm^{-1}	$\Delta\bar{\nu}_{0,1/2}$/cm^{-1}	S_m
1a	18750	1300	1900	1.45
1b	17150	1300	1850	1.25
1c	15970	1300	2400	1.2
1d	14850	1300	2400	0.85
2a	19400	1300	1890	1.4
2b	18350	1300	1800	1.25
2c	17700	1300	3200	1.12
2d	16800	1300	2460	1.6

[a] Estimated errors: $\Delta\bar{\nu}_{0,1/2}$ and S_m, ±10%; E_{oo} and $\hbar\omega_m$, ±5%.

There are some unique features that emerge from examination of the absorption spectra of the new complexes examined in this study. First, as shown in Figure 1, the MLCT absorption band red-shifts by nearly 3000 cm^{-1} over the series **1a** → **1d**. This red-shift is considerably larger than observed for a series of substituted (1,10-phenanthroline)Pt(−C≡C−Ar)$_2$ complexes[36] and is due to a very large difference in LUMO energies for the substituted 2,2′-bipyridine ligands in **1a**−**d**. Another point of interest is that in complexes **1c** and **1d** the low-energy MLCT feature clearly consists of two overlapping bands. This splitting suggests the possibility that there may be two orbitally distinct MLCT transitions, e.g., d_{xz}(Pt) → π^* (diimine) and d_{yz}(Pt) → π^* (diimine).

Photoluminescence. All of the (diimine)Pt(−C≡C−Ar)$_2$ complexes feature moderately intense photoluminescence (PL) at room temperature in fluid solution and at 80 K in a 2-MTHF glass. Example spectra are illustrated for complexes **1a** and **2b** in Figure 2. Table 1 lists the emission wavelength maxima at 298 K, as well as the thermally induced Stokes shifts (ΔE_s), which correspond to the difference in the 80 and 298 K emission energies. The room temperature emission spectra were fitted using a single-mode Franck−Condon expression (eq 1),

$$I(\bar{\nu}) = \sum_{\nu_m=0}^{5} \left\{ \left(\frac{E_{00} - \nu_m \hbar\omega_m}{E_{00}} \right)^3 \frac{(S_m)^{\nu_m}}{\nu_m!} \exp\left[-4 \ln 2 \left(\frac{\bar{\nu} - E_{00} + \nu_m \hbar\omega_m}{\Delta\bar{\nu}_{0,1/2}} \right)^2 \right] \right\} \quad (1)$$

where $I(\bar{\nu})$ is the relative emission intensity at energy $\bar{\nu}$, E_{00} is the energy of the zero−zero transition, ν_m is the quantum number of the average medium-frequency vibrational mode, $\hbar\omega_m$ is the average of medium-frequency acceptor modes coupled to the MLCT transition (1300 cm^{-1} was assumed throughout the series), S_m is the Huang−Rhys factor (i.e., the electron-vibration coupling constant), and $\Delta\bar{\nu}_{0,1/2}$ is the half-width of the individual vibronic bands. The parameters obtained by application of eq 1 for the complexes **1a**−**d** and **2a**−**d** are listed in Table 2, and fitted emission spectra are attached as Supporting Information. The parameters recovered from these spectral fits are used in a later section where a quantitative energy gap law analysis of the photophysical data for the complexes is considered.

Several features are worthy of note with respect to the PL spectra. First, the emission energy decreases substantially across series **1a**−**d**. At 298 K the emission energy of **1a** is 3900 cm^{-1} greater than that of **1d**. This large red shift is consistent with the PL emanating from a Pt → diimine MLCT state, since the emission energy decreases with the energy of the LUMO which is localized on the diimine acceptor ligand. Interestingly, the difference in E_{00} for **1b** and **1d** ($\Delta E_{00} = 2300$ cm^{-1}) is almost identical to that for (dcebpy)Re(CO)$_3$Cl and (dmb)Re(CO)$_3$Cl

($\Delta E_{00} = 2210$ cm^{-1}) (where dcebpy = 4,4′-dicarboethoxy-2,2′-bipyridine and dmb = 4,4′-dimethyl-2,2′-bipyridine).[14] This correlation points to the similarity in the nature of the emitting MLCT states for the d^8 Pt(II) and d^6 Re(I) systems. A second point of note is that all of the complexes **1a**−**d** feature large ΔE_s values. It has been shown that, for MLCT excited states, $\Delta E_s = 2\lambda_s$, where λ_s is the outer-sphere reorganization energy for the MLCT excited state.[16,17] Thus, we estimate that λ_s varies from 0.075 eV (**1a**) to 0.15 eV (**1b**−**d**). These comparatively large λ_s values indicate that there is a large difference between the dipole moments of the ground and MLCT excited states in the (diimine)Pt(−C≡C−Ar)$_2$ complexes. This is consistent with the findings of a transient DC photoconductivity study of the structurally related complex (Ph_2phen)Pt(S_2) (where Ph_2phen = 4,7-diphenylphenanthroline and S_2 is a dithiolate) which suggest that for this complex the ground-state dipole moment is ≈10 D and the dipole moment of the MLCT state is ≈0 D (i.e., $\Delta\mu = -10$ D).[51] In addition, the variable-temperature emission experiments on **1a**−**d** were carried out in 2-MTHF. This solvent is comparatively nonpolar, and consequently the λ_s values will be lower than if the studies were carried out in a more polar solvent such as EtOH/MeOH (this solvent mixture is commonly used for low-temperature spectroscopy of metal complexes).[16,17] By comparison, Ru(bpy)$_3^{2+}$ features a λ_s value of ≈ 0.05 eV in EtOH/MeOH solution.[52] This comparison suggests that the difference in dipole moments of the ground and MLCT excited states in **1a**−**d** is considerably larger than that of Ru(bpy)$_3^{2+}$.

The acetylide-substituted complexes **2a** and **2d** also feature comparatively large ΔE_s values (and by inference large λ_s), suggesting that the PL from these complexes also emanates from the Pt → diimine MLCT manifold. However, the situation is more complicated for **2b** and **2c**. Specifically, as shown in Figure 2, the emission energy for **2b** *decreases* with temperature down to 140 K, but below this temperature the emission energy *increases* with decreasing temperature. The net effect is that the emission energy of **2b** is virtually the same at 80 and 298 K. A qualitatively similar pattern is seen for **2c**. The lack of significant ΔE_s values for **2b** and **2c** clearly indicates that for these complexes the emission does not emanate from a MLCT manifold. Rather, we believe that for these two complexes the PL arises from a state having IL $^3\pi,\pi^*$ character. Additional evidence supporting this hypothesis is presented below.

The PL lifetimes and quantum yields (τ_{em} and ϕ_{em}, respectively) for all of the (diimine)Pt(−C≡C−Ar)$_2$ complexes in CH_2Cl_2 solution are listed in Table 1. The τ_{em} and ϕ_{em} values have also been used to compute radiative and nonradiative decay rate constants (k_r and k_{nr}, respectively), and these parameters are also compiled in the table. Several clear trends emerge from this data for complexes **1a**−**d**. Specifically, τ_{em} and ϕ_{em} decrease systematically with the emission energy. Inspection of the k_r and k_{nr} values for this series reveals that the energy gap dependence of τ_{em} and ϕ_{em} arises almost exclusively from variation in the nonradiative decay rate, i.e., k_{nr} increases almost 100-fold over the series **1a** → **1d**, while k_r varies randomly and by less than a factor of 4. The observed trend in k_{nr} is in accord with the energy gap law,[8,53] and a more thorough analysis of this trend is presented below.

In contrast to the behavior of **1a**−**d**, there are no clear trends in the ϕ_{em} and τ_{em} (or k_r and k_{nr}) values for **2a**−**d**, despite the fact that E_{00} varies by ≈2500 cm^{-1} across the series. The lack of a systematic trend in the photophysical parameters for the series points to the possibility that more than one excited state contributes to the photophysics of these complexes. The most obvious exception among the series **2a**−**d** is the $-NO_2$-substituted complex **2b**, which features a lifetime that is nearly 10-fold larger compared to the lifetimes of the other complexes. The large τ_{em} for **2b** arises because *both* k_r and k_{nr} are 10-fold lower compared to the values for the other complexes. Dramatically lower k_r and k_{nr} values have been reported for Ru(II) and Re(I) complexes where IL $^3\pi,\pi^*$ excited states are in close energetic proximity to the MLCT manifold,[54−56] and we suspect that a similar effect is manifest in complex **2b**. A more subtle, yet significant, deviation is seen in the photophysical parameters of the $-CF_3$-substituted complex **2a**. This complex features an unusually large k_{nr} value compared to the complexes in series **1a**−**d**, despite the fact that it has the highest emission energy of any of the (diimine)Pt(−C≡C−Ar)$_2$ complexes.

Transient Absorption Spectroscopy. Pulsed photoexcitation of the (diimine)Pt(−C≡C−Ar)$_2$ complexes with the 355 nm output of a Q-switched Nd:YAG laser affords transients that absorb relatively strongly throughout the near UV−visible region. Time-resolved absorption-difference (TA) spectra for all of the complexes (except **2c**, which features only a *very* weak TA spectrum) are illustrated in Figure 3, and the TA decay lifetimes (τ_{TA}) are listed in Table 1. For all of the complexes τ_{TA} and τ_{em} values are in excellent agreement, which implies that in each case the transient observed by absorption is the excited-state complex. (Another possibility is that the absorbing transient is in equilibrium with the emitting excited state.) The TA spectra of **1a**−**d** and **2d** are similar, with each spectrum featuring (1) a strong absorption band in the near UV ($\lambda_{max} \approx$ 360−370 nm); (2) bleaching or a "dip" in the 400−450 nm region; and (3) broad, moderately intense absorption throughout the visible region. These TA spectral features are hallmarks of metal → bipyridine MLCT excited states.[57−61] The strong near-UV and moderate visible absorptions arise from the bipyridine anion radical that is present in the MLCT state, i.e., (diimine$^{-\bullet}$)Pt^{III}(−C≡C−Ar)$_2$, and the "dip" that occurs in the 400−450 nm region is due to bleaching of the ground-state MLCT absorption band.[61] The MLCT assignment is further supported by the fact that the TA spectra of **1a**−**d** and **2d** are remarkably similar to those of the analogous (diimine)Re(CO)$_3$Cl complexes, which are known to feature lowest energy excited states based on the Re → diimine MLCT transition.[59,62]

A striking feature is that the TA spectra of complexes **2a** and **2b** are distinct from those of the remaining complexes. The TA spectrum of $-CF_3$-substituted complex **2a** features only a

(51) Vanhelmont, F. W. M.; Johnson, R. C.; Hupp, J. T. *Inorg. Chem.* **2000**, *39*, 1814−1816.
(52) Kitamura, N.; Kim, H.-B.; Kawanishi, Y.; Obata, R.; Tazuke, S. *J. Phys. Chem.* **1986**, *90*, 1488−1491.
(53) Caspar, J. V. Ph.D. Dissertation, University of North Carolina, Chapel Hill, NC, 1982.
(54) Shaw, J. R.; Webb, R. T.; Schmehl, R. H. *J. Am. Chem. Soc.* **1990**, *112*, 1117−1123.
(55) Shaw, J. R.; Schmehl, R. H. *J. Am. Chem. Soc.* **1991**, *113*, 389−394.
(56) Baba, A. I.; Shaw, J. R.; Simon, J. A.; Thummel, R. P.; Schmehl, R. H. *Coord. Chem. Rev.* **1998**, *171*, 43−59.
(57) Schanze, K. S.; Neyhart, G. A.; Meyer, T. J. *J. Phys. Chem.* **1986**, *90*, 2182−2193.
(58) Chen, P.; Westmoreland, T. D.; Danielson, E.; Schanze, K. S.; Anthon, D.; Neveaux, P. E., Jr.; Meyer, T. J. *Inorg. Chem.* **1987**, *26*, 1116−1126.
(59) MacQueen, D. B.; Schanze, K. S. *J. Am. Chem. Soc.* **1991**, *113*, 7470−7479.
(60) Sun, H.; Hoffman, M. Z.; Mulazzani, Q. G. *Res. Chem. Intermed.* **1994**, *20*, 735−754.
(61) Stufkens, D. J.; Vlcek, A. *Coord. Chem. Rev.* **1998**, *177*, 127−179.
(62) Schanze, K. S.; Macqueen, D. B.; Perkins, T. A.; Cabana, L. A. *Coord. Chem. Rev.* **1993**, *122*, 63−89.

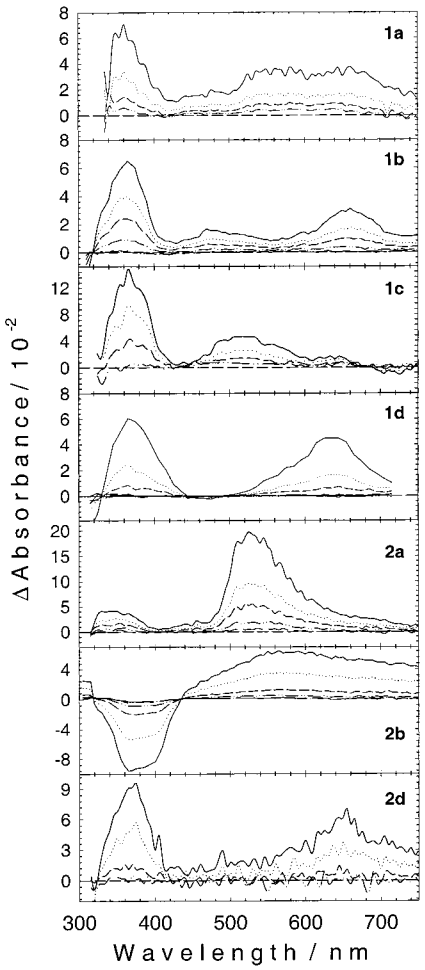

Figure 3. Transient absorption difference spectra for CH_2Cl_2 solutions at ambient temperature following 355 nm excitation. Spectra acquired at the following time increments (beginning immediately following the laser pulse): **1a**, 320 ns; **1b**, 320 ns; **1c**, 80 ns; **1d**, 80 ns; **2a**, 320 ns; **2b**, 4 μs; **2d**, 320 ns.

weak near-UV absorption, and the spectrum is dominated by a strong visible absorption band with $\lambda_{max} \approx 510$ nm. The spectrum of $-NO_2$-substituted complex **2b** is even more unique: it features strong bleaching in the region of the ground-state IL π,π^* absorption band ($\lambda \approx 370$ nm) and broad absorption throughout the visible and extending into the near-IR region. Although the assignment of excited states based on TA spectra is not without pitfalls, in the case of $-NO_2$ complex **2b** the shape of the TA spectrum clearly signals that the excited state involves the nitro-substituted aryl acetylide ligands ($-C\equiv C-Ar-NO_2$). There are two possibilities for the lowest excited state that is observed by TA spectroscopy: (1) a $^3\pi,\pi^*$ state that is localized on the $-C\equiv C-Ar-NO_2$ ligands; (2) a Pt $\rightarrow$ $C\equiv C-Ar-NO_2$ MLCT excited state. We favor the former assignment based on the fact that the TA spectrum of **2b** is very similar to that of conjugated phenylene ethynylenes (i.e., $[-C\equiv C-Ar-]_x$) and complexes of the type *trans*-$Pt(PR_3)_2(-C\equiv C-Ar)_2$, which are known to feature lowest $^3\pi,\pi^*$ excited states.[63−65] For example, the transient absorption of the $^3\pi,\pi^*$ state of the complex *trans*-$(Bu_3P)_2Pt(-C\equiv C-$t-St$)_2$ (where t-St is *trans*-stilbene) features a strong ground-state bleach at 375 nm along with a broad absorption that extends throughout the visible (see Supporting Information).[64] Although assignment of the TA spectrum of $-CF_3$-substituted complex **2a** is less clear, the presence of the strong mid-visible transient absorption band suggests that the lowest excited state in this complex may also have IL $^3\pi,\pi^*$ character.

Time-Resolved Infrared Spectroscopy. The method of fast time-resolved infrared spectroscopy is invaluable for probing the vibrational and electronic structure of excited states and reactive intermediates formed by photoexcitation of transition metal organometallic complexes.[66−69] The technique is particularly useful when applied to complexes featuring ligands that absorb strongly in the IR (e.g., CO and CN) and when the excited states are MLCT in nature.[66,70,71] For example, in complexes of the type (diimine)$Re^I(CO)_3(L)$, (diimine)$_2Os^{II}$-(CO)(L), and $W(CO)_5$(pyridine-X), the CO vibrational absorption band(s) undergo(es) a significant shift to higher frequency in the excited state.[66,70,71] The shifts to higher frequency are attributed to the fact that MLCT excitation effectively decreases the electron density at the metal center, resulting in decreased M $\rightarrow$ CO back-bonding. By contrast, complexes that feature metal-centered or intraligand excited states typically exhibit very little shift in the frequency of the CO bands.[69]

In order to gain further insight into the electronic structure of the excited states of the (diimine)Pt$(-C\equiv C-Ar)_2$ complexes, time-resolved step-scan FTIR spectroscopy (s^2-FTIR) was used to probe the shifts in the $\nu(C\equiv C)$ IR bands upon formation of the excited state. In the MLCT excited state the decrease in electron density that occurs at the Pt center due to Pt $\rightarrow$ diimine MLCT should be reflected by an increase in the frequency of the acetylide stretching band(s).

Figure 4a shows the ground-state FTIR spectrum of **1a** in CH_2Cl_2. There are two $\nu(C\equiv C)$ bands at 2115 and 2124 (sh) cm^{-1}. Figure 4b shows the s^2-FTIR difference spectrum of this solution obtained 50 ns after irradiation (355 nm). The parent IR bands are bleached, and a new excited-state band is produced at 2142 cm^{-1}. Under the higher concentration used in the s^2-FTIR experiments, the excited-state lifetime is 420 ns. In principle there should be two excited-state bands produced. However, only one strong absorption is resolved. This may be due to an accidental overlap of the two excited-state bands, or the second band may not be resolved due to the signal-to-noise of the data.

The s^2-FTIR spectra of **1b** in CH_2Cl_2 at 298 K and in a PrCN/BuCN glass at 77 K were also characterized, and these spectra are shown in Figure 4c. The room temperature s^2-FTIR of **1b** shows features that are similar to those of **1a**. In both **1a** and **1b**, the excited-state $\nu(C\equiv C)$ IR band is shifted ca. 30−35 cm^{-1} relative to the mean band position of the ground-state absorptions.

The shift of the $\nu(C\equiv C)$ bands to higher frequency is consistent with the MLCT character of the excited states of **1a** and **1b**, i.e., the decreased (dπ) Pt $\rightarrow$ (π^*) $-C\equiv C-Ar$ back-

(63) Walters, K. A.; Ley, K. D.; Schanze, K. S. *J. Chem. Soc., Chem. Commun.* **1998**, *10*, 1115−1116.
(64) Glusac, K.; Schanze, K. S. Unpublished.
(65) Cooper, T. M.; McLean, D. G.; Rogers, J. E. *MRS Symp. Proc.*, in press.
(66) Turner, J. J.; George, M. W.; Johnson, R. C.; Westwell, J. R. *Coord. Chem. Rev.* **1993**, *125*, 101−114.
(67) Gamelin, D. R.; George, M. W.; Glyn, P.; Grevels, F.-W.; Johnson, F. P. A.; Klotzbucher, W.; Morrison, S. L.; Russell, G.; Schaffner, K.; Turner, J. J. *Inorg. Chem.* **1994**, *33*, 3246−3250.
(68) Clark, I. P.; George, M. W.; Johnson, F. P. A.; Turner, J. J. *Chem. Commun.* **1996**, 1587−1588.
(69) Schoonover, J. R.; Strouse, G. F.; Dyer, R. B.; Bates, W. D.; Chen, P.; Meyer, T. J. *Inorg. Chem.* **1996**, *35*, 273−274.
(70) Schoonover, J. R.; Bignozzi, C. A.; Meyer, T. J. *Coord. Chem. Rev.* **1997**, *165*, 239−266.
(71) Schoonover, J. R.; Strouse, G. F. *Chem. Rev.* **1998**, *98*, 1335−1355.

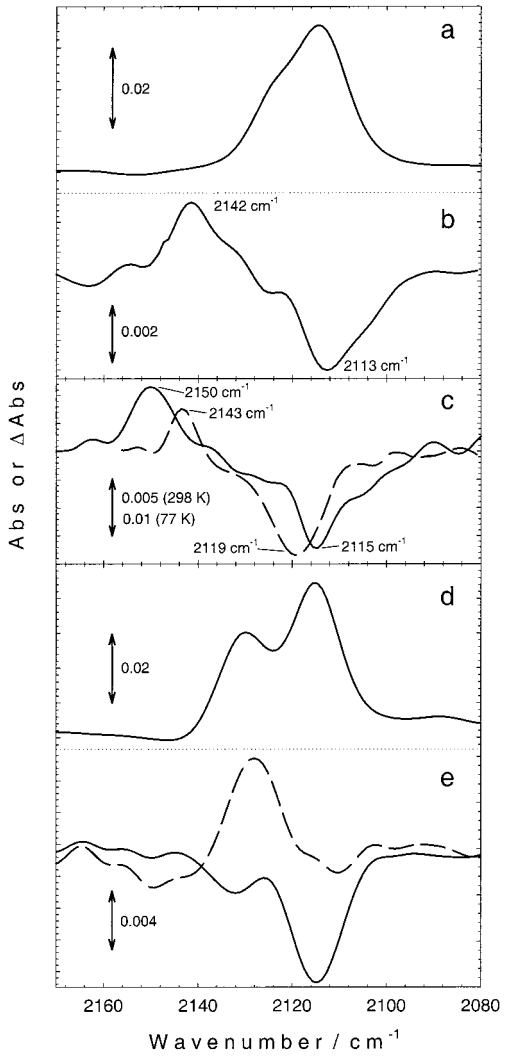

Figure 4. Ground- and excited-state infrared spectra for complexes **1a**, **1b**, and **2b**. (a) Ground-state FTIR spectrum of **1a** in CH_2Cl_2 solution at 298 K. (b) s^2-FTIR difference spectrum for **1a** in CH_2Cl_2 solution at 298 K 50 ns after excitation. (c) s^2-FTIR difference spectra of **1b**. Solid line: 298 K in CH_2Cl_2 solvent. Dashed line: 77 K in BuCN/PrCN (5:4 v:v) solvent glass. (d) Ground-state FTIR spectrum of **2b** in BuCN/PrCN (5:4 v:v) solvent glass at 77 K. (e) s^2-FTIR spectra for **2b** in BuCN/PrCN (5:4 v:v) solvent glass 77 K 50 ns after excitation. Solid line: difference spectrum. Dashed line: calculated excited-state absorption spectrum.

bonding that is expected concomitant with Pt → diimine charge transfer. The s^2-FTIR spectrum of complex **1b** was also obtained in a BuCN/PrCN (5:4 v:v) glass at 77 K (dashed line in Figure 4c). Interestingly, $\Delta\bar{\nu}_{C\equiv C}$ is considerably less in the glass (+24 cm^{-1}) compared to the value in solution. A similar effect was previously reported for the complex $(bpy)Re^{I}(CO)_3Cl$, and in this system $\Delta\bar{\nu}_{C\equiv O}$ was significantly lower for the each of the three C≡O bands.[68] The decreased $\Delta\bar{\nu}$ seen in the glass has been termed "infrared rigidochromism" and is clearly associated with the rigidity of medium (as opposed to being simply due to the low temperature), but the mechanism for effect is not fully understood.[68]

It is also of interest to compare the room temperature $\Delta\bar{\nu}_{C\equiv C}$ values for **1a** and **1b** with shifts seen for CO ligands in MLCT excited-state complexes. The most extensive work in this area has centered on complexes of the type $(diimine)Re^{I}(CO)_3(L)$, and in these systems $\Delta\bar{\nu}_{C\equiv O}$ is typically +60 cm^{-1} in the Re → diimine MLCT state.[67,68,70] Studies have also examined the shift in the MLCT excited state of complexes of the type $(diimine)_2Os^{II}(CO)(L)$, and in this case $\Delta\bar{\nu}_{C\equiv O} \approx +70$ cm^{-1} is typical.[70,71] It is clear from this comparison that $\Delta\bar{\nu}_{C\equiv C}$ in **1a** and **1b** is substantially less than is typical for $\Delta\bar{\nu}_{C\equiv O}$ in M → diimine MLCT states. Given that the extent of π-back-bonding in metal−acetylide complexes is considerably less than in CO complexes, a priori we anticipate that the C≡C bond will be less sensitive to the change in electron density that is induced by MLCT excitation.[72] This is likely the primary reason that $\Delta\bar{\nu}_{C\equiv C}$ is less than $\Delta\bar{\nu}_{C\equiv O}$ for MLCT excited states. An additional contributing factor leading to the lower $\Delta\bar{\nu}_{C\equiv C}$ values observed for the bis-acetylide complexes is that the acetylide-based π^* orbital(s) are more highly delocalized than the π^* CO orbitals in the carbonyl complexes (e.g., the acetylide-based π^* orbitals are delocalized into the aromatic rings). This delocalization may attenuate the effect of decreased (dπ) Pt → (π^*) −C≡C−Ar back-bonding on the C≡C stretching frequency.

In distinct contrast to the s^2-FTIR spectra of **1a** and **1b**, the spectrum of **2b** (5:4 BuCN/PrCN, glass at 77 K) features only depletion of the parent absorption without formation of any strong new bands (Figure 4e, solid line). The two ground-state IR bands of **2b** are well separated (Figure 4d, 2115 and 2130 cm^{-1}), and careful inspection of the parent depletion shows that the intensity ratio of the bleaches is different from their ratio in the ground-state FTIR spectrum. Subtraction of the ground-state spectrum of **2b** from its s^2-FTIR spectrum affords the excited-state absorption spectrum (Figure 4e, dashed line) that features a single band at 2128 cm^{-1}. This excited-state spectrum implies that there is a very small $\Delta\bar{\nu}_{C\equiv C}$ in **2b,** which in turn suggests that there is significantly less charge-transfer character in the complex's excited state. This is clearly consistent with an IL $^3\pi,\pi^*$ assignment for the excited state of **2b**.[69] It has been previously shown that in metal−carbonyl complexes which feature an IL $^3\pi,\pi^*$ excited state $\bar{\nu}_{C\equiv O}$ shifts slightly to lower frequency relative to the ground state.[69] The small increase in $\bar{\nu}_{C\equiv C}$ seen in the exited state of **2b** may arise because in the $^3\pi,\pi^*$ excited state the C≡C bond order is slightly diminished due to increased π-conjugation between the C≡C bonds and the phenyl rings.

Quantitative Analysis of Nonradiative Decay. Extensive studies have been carried out to demonstrate that the nonradiative decay rates of MLCT excited states in transition metal complexes can be accurately modeled using nonradiative decay theory.[8,13,73−77] Specifically, it has been shown that for series of structurally related polypyridine complexes of Os(II),[13,77] Re(I),[14] and Ru(II)[78] the nonradiative decay rate decreases exponentially as the energy of the MLCT states increases. This effect is termed the energy gap law, and the most often used

(72) The fact that back-bonding is not particularly strong is evidenced by the fact that the ground-state $\bar{\nu}_{C\equiv C}$ is nearly the same for the (diimine)-Pt(−C≡C−Ar)$_2$ complexes and free phenylacetylene ($\bar{\nu}_{C\equiv C}$ = 2124 cm^{-1}).

(73) Robinson, G. W.; Frosch, R. P. *J. Chem. Phys.* **1963**, *38*, 1187−1203.
(74) Siebrand, W. *J. Chem. Phys.* **1967**, *46*, 440−447.
(75) Siebrand, W. *J. Chem. Phys.* **1966**, *44*, 4055−4057.
(76) Avouris, P.; Gelbart, W. M.; El-Sayed, M. A. *Chem. Rev.* **1977**, *77*, 793−834.
(77) Kober, E. M.; Caspar, J. V.; Lumpkin, R. S.; Meyer, T. J. *J. Phys. Chem.* **1986**, *90*, 3722−3734.
(78) Barqawi, K. R.; Murtaza, Z.; Meyer, T. J. *J. Phys. Chem.* **1991**, *95*, 47−50.

expression to analyze nonradiative decay rate data is[77]

$$\ln k_{nr} = \ln \beta_o - \frac{\gamma_o E_{00}}{\hbar\omega_m} - S_m + (\gamma_o + 1)^2 \frac{(\Delta\bar{\nu}_{0,1/2}/\hbar\omega_m)^2}{16 \ln 2} - 0.5 \ln\left(\frac{\hbar\omega_m E_{00}}{1000\ \mathrm{cm}^{-1}}\right) \quad (2a)$$

$$\beta_o = |C_k|^2 \omega_k \left(\frac{\sqrt{\pi/2}}{1000\ \mathrm{cm}^{-1}}\right) \quad (2b)$$

$$\gamma_o = \ln\left(\frac{E_{00}}{\hbar\omega_m S_m}\right) - 1 \quad (2c)$$

where S_m, E_{00}, $\Delta\bar{\nu}_{0,1/2}$, and $\hbar\omega_m$ are the same terms defined in eq 1, β_o is the vibronically induced electronic coupling term, C_k is the vibronic coupling matrix element, and ω_k is the frequency of the promoting vibrational mode (i.e., the mode that mixes the ground and excited electronic states). Two simplifications of eqs 2a−c are possible which facilitate analysis of experimental data.[77] First, under the assumption that all but the second term on the right-hand side (rhs) of eq 2a are nearly invariant with E_{00} leads to eq 3a, which predicts that the log of the nonradiative decay rate will vary linearly with E_{00}. This equation is the mathematical statement of the energy gap law. Alternatively, noting that all but the first term on the rhs in eq 2a can be calculated by fitting the photoluminescence spectra by using eq 1 suggests that eq 2a can be recast as eq 3b where the last four terms are represented by a single term, ln[FCF(calcd)] (where FCF(calcd) is an abbreviation for "calculated Franck−Condon factors").

$$\ln k_{nr} = a - \left(\frac{\gamma_o}{\hbar\omega_m}\right) E_{00} \quad (3a)$$

$$\ln[\mathrm{FCF(calcd)}] = \ln k_{nr} - \ln \beta_o \quad (3b)$$

Equation 3a implies that a plot of ln k_{nr} vs E_{00} will be linear with slope $= \gamma_o/\hbar\omega_m$, while eq 3b suggests that a plot of ln[FCF(calcd)] vs ln k_{nr} will be linear with a slope $= 1.0$ and an intercept of $-\ln \beta_o$.

Eisenberg and co-workers noted that the nonradiative decay rates for their series of (diimine)Pt(−C≡C−Ar)$_2$ complexes obeyed the energy gap law,[36] but due to the relatively small range of E_{00} values accessed by their series it is not possible to apply quantitative energy gap law models to analyze the rate data. As noted above, the E_{00}'s for complexes **1a**−**d** and **2a**−**d** span a wide energy range, making it possible to apply eqs 3a and 3b, along with the parameters recovered from the photoluminescence spectral fitting procedure, to assess how well the nonradiative decay rates for the series are modeled by theory.

As noted above, the room temperature photoluminescence spectra of **1a**−**d** and **2a**−**d** were fitted using eq 1, and the parameters recovered from those fits are reported in Table 2. All of the spectra were fitted assuming a dominant acceptor mode of 1300 cm^{-1}. (This choice is based on the idea that C−C diimine skeletal vibrations are the dominant acceptor modes, and is supported by the observation of a resolved vibronic progression in the low-temperature emission spectra, e.g., Figure 2, top.) The other parameters were varied to optimize the fits (see Supporting Information for the fitted spectra). One point of note is that, in general, S_m increases with E_{00}; correlation between S_m and E_{00} has been observed in other series of MCLT states[14,77] and has been attributed to the fact that the extent of charge transfer in the MLCT state increases with E_{00}.

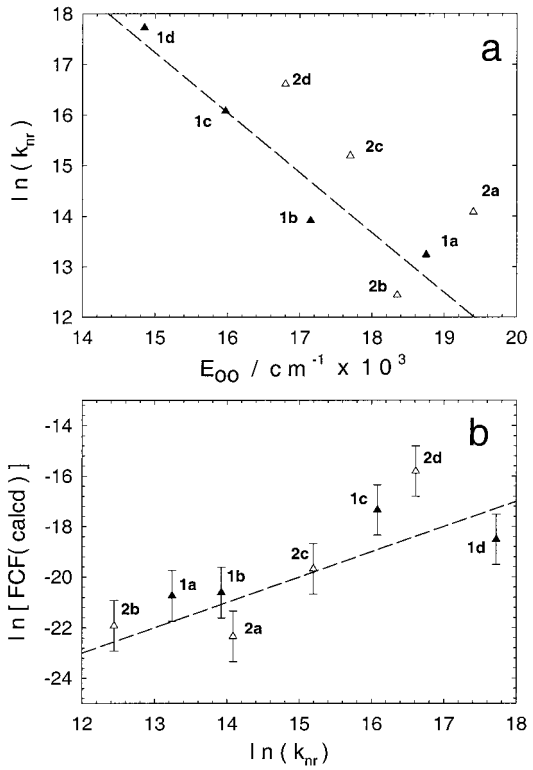

Figure 5. Energy gap law analysis for the (diimine)Pt(−C≡C−Ar)$_2$ complexes in CH_2Cl_2 solution at 298 K. (a) Plot of ln k_{nr} versus E_{00}. (b) Plot of ln[FCF(calcd)] versus ln k_{nr}. Closed triangles: data for series **1a**−**d**. Open triangles: data for series **2a**−**d**.

Figure 5a illustrates the correlation of ln k_{nr} vs E_{00} for the series of complexes **1a**−**d** and **2a**−**d**. As can be seen from this plot, the data for the series in which only the bipyridine ligand is substituted (**1a**−**d**) follow a reasonable linear correlation. The dashed line is a linear least-squares fit of the data for complexes **1a**−**d** with slope, $\delta(\ln k_{nr})/\delta(E_{00}) = -1.18 \times 10^{-3}$ cm^{-1}. By contrast, the data for the series in which the aryl acetylide ligand is varied clearly does not follow the same energy gap correlation. In addition, the point for $-NO_2$-substituted complex **2b** is markedly skewed from any correlation. (Note that this complex has already been identified as the most likely to have a lowest $^3\pi,\pi^*$ excited state.) The slope of the energy gap law correlation for **1a**−**d** is consistent with the premise that the dominant acceptor mode has $\hbar\omega_m \approx 1300$ cm^{-1}, since by using this value for $\hbar\omega_m$ we compute a slope that is in good agreement with the least-squares slope (i.e., $\gamma_o/\hbar\omega_m \approx 1.16 \times 10^{-3}$ cm^{-1}).[79] This is significant, because it implies that the C≡C stretch does not play a significant role in accepting the energy that is released concomitant to nonradiative decay of the MLCT state (i.e., a larger $\delta(\ln k_{nr})/\delta(E_{00})$ would be expected if the C≡C stretch operates as an acceptor mode). Interestingly, $\delta(\ln k_{nr})/\delta(E_{00})$ is in reasonable agreement with the value obtained from an energy gap law analysis of nonradiative decay rates for the series of complexes (X_2-bpy)Re^I(CO)$_3$Cl, where $(\delta(\ln k_{nr})/\delta(E_{00}) = 0.91 \times 10^{-3}$ cm^{-1}. This correspondence underscores the similarity in the structure of the MLCT states in the (diimine)Re^I(CO)$_3$Cl and (diimine)Pt(−C≡C−Ar)$_2$ systems, and also suggests that the carbonyl and acetylide ligands play similar (and marginal) roles in the MLCT photophysics of the chromophores. Also of

(79) γ_0 is computed by using eq 2c, assuming $\hbar\omega_m = 1300$ cm^{-1} and $S_m = 1.0$.

interest is the fact that there is good agreement in the energy gap law correlation for the (diimine)Pt($-$C≡C$-$Ar)$_2$ complexes and a series of (diimine)Pt(tdt) complexes, where tdt = 2,3-toluenedithiolate.[30] This similarity further underscores the small role played by the acetylide ligands in the MLCT photophysics of the complexes.

Finally Figure 5b presents a correlation of ln[FCF(calcd)] vs ln k_{nr} for complexes **1a**$-$**d** and **2a**$-$**d**. The dashed line has slope = 1.0 and intercept = -35 (note eq 3b). While the correlation is not outstanding, there is at least a qualitative agreement for the series of complexes. The intercept of the correlation suggests a value of $\beta_0 = 5.8 \times 10^{14}$ cm^{-1}. This vibronically induced electronic coupling term that is estimated for the (diimine)Pt($-$C≡C$-$Ar)$_2$ complexes is in excellent agreement with values of β_o recovered from energy gap analysis of several series of Ru(II), Os(II), and Re(I) polypyridyl complexes, where values of β_o ranging from 1.3×10^{14} to 5.8×10^{14} cm^{-1} have been estimated.

Excited-State Scheme for the (diimine)Pt($-$C≡C$-$Ar)$_2$ Complexes. Consideration of the spectroscopic data presented above for the diimine platinum acetylide complexes makes it evident that there are two manifolds of excited states that play a role in their photophysics. First, there is a set of ^{1}MLCT and ^{3}MLCT states which derive from the dπ (Pt) → π^* (diimine) transition. The existence of the MLCT manifold is clear: in most of the complexes the low-energy absorption is dominated by the allowed transition to the ^{1}MLCT state, while the photoluminescence, transient absorption, and s^2-FTIR spectroscopy are dominated by the long-lived ^{3}MLCT state. For the series of complexes the energies of the ^{1}MLCT states lie in the range 2.8$-$3.3 eV (as estimated from the position of the allowed MCLT absorption band). More importantly, the long-lived ^{3}MLCT state falls in the energy range 1.85$-$2.4 eV, depending upon the substituents on the diimine and aryl acetylide ligands.

In addition to the IL π,π^* states that are based on the diimine ligand, each complex also features a manifold of IL π,π^* states based on transitions between π and π^* orbitals localized largely upon the aryl acetylide ligands (i.e., $^1\pi,\pi^*_{C\equiv CAr}$ and $^3\pi,\pi^*_{C\equiv CAr}$). In most of the complexes the optical transition to the $^1\pi,\pi^*_{C\equiv CAr}$ state is obvious: there is an intense band ($\epsilon \approx 5 \times 10^4$ M^{-1} cm^{-1}) in the absorption spectra in the 290$-$300 nm region. This transition places the energy of the $^1\pi,\pi^*_{C\equiv CAr}$ state in the region of 3.8$-$4.0 eV. Several points are of interest with respect to this absorption. First, the aryl acetylide based π,π^* absorption occurs at a longer wavelength (lower energy) compared to the absorption bands of the corresponding free aryl acetylenes.[80] This shift to lower energy implies that there is an interaction between the π electron systems of the two aryl acetylide ligands, and this interaction leads to a decrease in the energy of the $\pi,\pi^*_{C\equiv CAr}$ manifold. Second, it is obvious that the aryl acetylide based π,π^* absorption band is shifted to considerably lower energy in complex **2b**. On the basis of the position of this band, the energy of the $^1\pi,\pi^*_{C\equiv CAr}$ state in this complex is ≈3.3 eV. This considerable red shift of the band may be due to mixing of some Pt → C≡C$-$Ar$-$NO$_2$ charge-transfer character into the transition. However, we believe that, despite the existence of some charge-transfer character, the excited state that derives from this transition retains the characteristics of a π,π^* excited state. This conjecture is based on the observation that the emission from this complex (which arises from the $^3\pi,\pi^*_{C\equiv CAr}$ state, see below) does not vary in energy significantly with temperature (i.e., the rigidochromic effect, which is characteristic of charge-transfer emission, is absent).

The $^3\pi,\pi^*_{C\equiv CAr}$ state is more important than the $^1\pi,\pi^*_{C\equiv CAr}$ state with respect to the excited-state spectroscopy and decay kinetics of the complexes. However, in order for the $^3\pi,\pi^*_{C\equiv CAr}$ state to have a significant influence, it must be no greater than a few hundred millielectronvolts higher in energy than the ^{3}MLCT state. On the basis of singlet$-$triplet splittings typical of organic aromatic hydrocarbons (1.2$-$1.5 eV),[81,82] we predict that for $-$NO$_2$-substituted complex **2b**, the $^3\pi,\pi^*_{C\equiv CAr}$ state lies in the energy range 1.8$-$2.1 eV, and for the remaining complexes the $^3\pi,\pi^*_{C\equiv CAr}$ state lies between 2.5 and 2.7 eV. The existence of this low-lying $^3\pi,\pi^*_{C\equiv CAr}$ state has important consequences for the photophysics of the (diimine)Pt($-$C≡C$-$Ar)$_2$ complexes. First, for complexes **1a**$-$**d** it is clear that ^{3}MLCT is the lowest excited state. In each case the available photophysical data are in accord with a ^{3}MLCT assignment. Second, for **2b**, it is evident that $^3\pi,\pi^*_{C\equiv CAr}$ is lower energy than ^{3}MLCT. The transient absorption, photoluminescence, and s^2-FTIR spectra of this complex are distinctly different from those of **1a**$-$**d**, and its excited-state decay rate parameters (i.e., k_r and k_{nr}) are considerably less than those for the other complexes. The situation regarding the nature of the lowest excited state is less clear for complexes **2a**, **2c**, and **2d**. Specifically, the transient absorption of complex **2a** is not typical for a ^{3}MLCT state, but its excited-state decay rate parameters are "normal". We conclude that in this complex the ^{3}MLCT state is pushed to a relatively high energy (because of the electron-withdrawing $-$CF$_3$ groups) bringing it close in energy to $^3\pi,\pi^*_{C\equiv CAr}$. In this case, the two excited states may be in equilibrium, which would explain the discontinuity between the transient absorption spectrum (which suggests $^3\pi,\pi^*_{C\equiv CAr}$) and the decay rate parameters (which are indicative of ^{3}MLCT).[56,83,84] The photophysics of $-$OCH$_3$-substituted complex **2d** appears to be rather typical for an unperturbed ^{3}MLCT state. By contrast, the $-$N(CH$_3$)$_2$-substituted complex is unusual, since it features a *negative* ΔE_s (Table 1), very weak emission at room temperature, and no easily observable transient absorption. The excited-state scheme for this complex may be the most complicated of the entire series, since, in addition to the MLCT and $\pi,\pi^*_{C\equiv CAr}$ manifolds, this complex likely also features a low-energy ligand-to-ligand charge-transfer (LLCT) state based on charge transfer from the $-$N(CH$_3$)$_2$-substituted acetylide ligand to the diimine acceptor.[85,86]

Conclusion

A comprehensive photophysical investigation has been carried out on a series of eight (diimine)Pt($-$C≡C$-$Ar)$_2$ complexes. Series **1a**$-$**d**, which feature a fixed aryl acetylide (*p*-tolylacetylene) and a series of diimine ligands with varying electron demand, have a low-lying ^{3}MLCT excited state which dictates the complexes' photophysics. The ^{3}MLCT assignment is

(80) Younis, M.; Long, N. J.; Raithby, P. R.; Lewis, J.; Page, N. A.; White, A. J. P.; Williams, D. J.; Colbert, M. C. B.; Hodge, A. J.; Khan, M. S.; Parker, D. G. *J. Organomet. Chem.* **1999**, *578*, 198$-$209.

(81) Görner, H. *J. Phys. Chem.* **1989**, *93*, 1826$-$1832.

(82) Murov, S. L.; Carmichael, I.; Hug, G. L. *Handbook of Photochemistry*, 2nd ed.; Marcel Dekker: New York, 1993.

(83) Simon, J. A.; Curry, S. L.; Schmehl, R. H.; Schatz, T. R.; Piotrowiak, P.; Jin, X.; Thummel, R. P. *J. Am. Chem. Soc.* **1997**, *119*, 11012$-$11022.

(84) Schmehl, R. H. *The Spectrum* (Newsletter of the Center for Photochemical Sciences, Bowling Green State University, http://www.bgsu.edu/departments/photochem/) **2000**, *13*, 17$-$21.

(85) Perkins, T. A.; Humer, W.; Netzel, T. L.; Schanze, K. S. *J. Phys. Chem.* **1990**, *94*, 2229$-$2232.

(86) Perkins, T. A.; Pourreau, D. B.; Netzel, T. L.; Schanze, K. S. *J. Phys. Chem.* **1989**, *93*, 4511$-$4522.

supported by optical transient absorption and s^2-FTIR spectroscopy. In addition, the nonradiative decay rates for series **1a**−**d** adhere quantitatively to an energy gap law correlation. Analysis of the correlation indicates that the electronic and vibronic characteristics of the Pt → diimine MLCT state are remarkably similar to that of the Re → diimine MLCT state in complexes of the type (diimine)$Re^{I}(CO)_3$(L). The photophysical properties of series **2a**−**d**, which feature a fixed diimine acceptor ligand (4,4′-bis(*tert*-butyl)-2,2′-bipyridine) along with a series of aryl acetylide ligands with varying electron demand, are more complicated. The photophysical rate parameters for these complexes fit an energy gap law correlation only qualitatively; in addition, several of the complexes feature unusual transient absorption and photoluminescence spectral characteristics. This leads to the conclusion that for at least some of these complexes the $^3\pi,\pi^*_{C\equiv CAr}$ state is close in energy to the ^{3}MLCT state and plays a major role in determining the photophysical properties of the complexes.

Acknowledgment. This work was supported by grants from the National Science Foundation (CHE-9901861) and the Royal Society (J.A.W.). We also acknowledge Dr. Yao Liu for obtaining optical absorption spectra. We also acknowledge helpful comments from Prof. R. Eisenberg and the reviewers regarding interpretation of the experimental data.

Supporting Information Available: A figure showing the room temperature emission spectra of all of the complexes in CH_2Cl_2 solution along with the fitted spectra computed using eq 1 and the parameters shown in Table 2. A figure showing the transient absorption spectrum of *trans*-$(Bu_3P)_2Pt(-C\equiv C-t\text{-}St)_2$. This material is available free of charge via the Internet at http://pubs.acs.org.

IC0102182